monuclear scalar coupling was best determined with the standard two-dimensional COSY experiment with 2K complex points in t_2, 1K points in the t_1 domain, and a recycle delay of >2 s in addition to the acquisition time. The two-dimensional phase-sensitive NOESY was acquired with 4K data points in the t_2 dimension, 1K data points in t_1, and a recycle delay of >2 s in addition to the acquisition time.[27,28] Mixing times of 250 and 500 ms were used that were stochastically varied to suppress cross-peaks arising from scalar coupling. A shifted sine bell multiplication apodization of 45% was applied in the t_2 and t_1 domains. ^{1}H-Decoupled ^{31}P spectra were collected at 202.44 MHz, and ^{1}H-^{31}P correlation experiments were performed according to the procedure described by Bax et al.[29]

Molecular Modeling Studies. The crystal structure of **1b** was used as the initial structure in this investigation. Partial atomic charges for anthramycin with the methoxy group removed were provided by Rao et al.[15] Bond length, bond angle, and dihedral parameters for the all atom force field were those presented by Weiner et al.,[31,32] and new parameters specific to anthramycin were given by Rao et al.[15] The resulting structure was minimized with the program AMBER[31] with a distance-dependent dielectric constant, and refinement continued until the rms gradient was less than 0.1 kcal/mol·Å. This minimized structure was docked in the appropriate location and orientations on the hexanucleotide duplex with the aid of the interactive graphics program MIDAS,[33] and then the binding energies were minimized with AMBER and the parameters described above. The helix energy was determined by subtracting the energy of the helix in the anthramycin adduct from that of the separately minimized isolated helix. Distortion energy induced in the anthramycin molecule was determined in the same way.

Structural effects of water and counterions on complexing were neglected in the energy calculations. Although these effects influence the absolute values of binding energies, they should be minimal in comparing relative binding energies wherein the same molecule is used at the same binding site on the duplex.

Acknowledgment. This work was supported by grants from the NIH (GM-22873), National Cancer Institute (R35-CA-49751 and CA-37798), and Welch Foundation. We thank Joann Haddock for her patience in preparing this manuscript. We also thank Shashidhar N. Rao for data on anthramycin and helical distances, Dr. Peter A. Kollman for a copy of AMBER, and Professor Thomas Krugh for unpublished results and useful discussions.

(28) States, D. J.; Habverkorn, R. A.; Ruben, D. J. *J. Magn. Reson.* **1982**, *48*, 286.
(29) Bax, A.; Sarkar, S. K. *J. Magn. Reson.* **1984**, *60*, 170.
(30) Weiner, S. J.; Kollman, P. A.; Case, D.; Singh, U. C.; Ghio, C.; Alagona, G.; Profeta, S., Jr.; Weiner, P. K. *J. Am. Chem. Soc.* **1984**, *106*, 765.
(31) Weiner, S. J.; Kollman, P. A.; Nguyen, D. T.; Case, D. A. *J. Comp. Chem.* **1986**, *7*, 230.
(32) Weiner, P. K.; Kollman, P. A. *J. Comp. Chem.* **1984**, *2*, 287.
(33) Langridge, R.; Ferrin, T. *J. Mol. Graphics* **1984**, *2*, 56.

Resonance Raman Spectra of Reaction Intermediates in the Oxidation Process of Ruthenium(II) and Iron(II) Porphyrins

Insook Rhee Paeng and Kazuo Nakamoto*

Contribution from the Todd Wehr Chemistry Building, Marquette University, Milwaukee, Wisconsin 53233. *Received June 15, 1989*

Abstract: The dioxo ruthenium porphyrins, $RuP(O)_2$ (P = TPP and TMP), were prepared by the oxidation of RuP(CO) with *m*-chloroperoxybenzoic acid (*m*-CPBA). The resonance Raman and IR spectra of $RuP(O)_2$ were measured and their O=Ru=O vibrations including the ^{16}O=Ru=^{18}O and ^{18}O=Ru=^{18}O analogues assigned by normal coordinate calculations. A reaction scheme involving two successive O—O bond cleavages of *m*-CPBA was proposed based on the observed intensity patterns of the O=Ru=O vibrations. When a toluene solution of Ru(TPP) was saturated with O_2 at -80 °C, the ν_s(Ru-O) of (TPP)Ru-O-O-Ru(TPP) was observed at 552 cm^{-1} (533 cm^{-1} for the ^{18}O analogue). Upon raising the temperature, this band disappeared, and the ν_s(O=Ru=O) of Ru(TPP)$(O)_2$ appeared at 811 cm^{-1} (767 cm^{-1} for the ^{18}O analogue). The ν(RuO) of the monoxo complex, O=Ru(TPP), was observed at 780 cm^{-1} when a toluene-d_8 solution of Ru(TPP) was saturated with $^{18}O_2$ at -80 °C. Similar experiments with Ru(OEP) exhibited the ν(RuO) at 820 cm^{-1} (779 cm^{-1} for the ^{18}O analogue). Bands characteristic of the Ru—O—O—Ru bridge and O=Ru=O moiety were not observed for the OEP complex. The six-coordinate, Ru(TPP)(pyridine)O_2 exhibits the ν(Ru—O_2) at 603 cm^{-1}, which is higher than the ν(Fe—O_2) of the corresponding Fe complex (575 cm^{-1}). The resonance Raman spectra of PFe—O—O—FeP and O=FeP (P = TPP, OEP, and other porphyrins), which are formed in the oxidation process of these Fe porphyrins, have been measured including the high-frequency region. In all cases, the peroxo-bridged species and the ferryl species are present at low temperature, and the former is converted into the latter by raising the temperature.

Considerable attention has been given to the interactions between dioxygen and low-valent metalloporphyrins because of their relevance to biological systems. In particular, the reactions of iron porphyrins with dioxygen[1-10] have been studied extensively in the past decade. Recently, the reactions of ruthenium porphyrins with dioxygen have also received considerable attention.

Scheme I

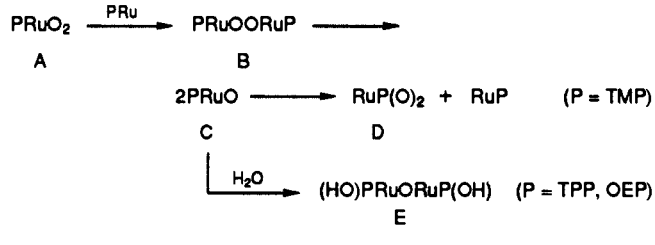

(1) Spiro, T. G. In *Iron Porphyrins*; Lever, A. B. P., Gray, H. B., Eds.; Addison-Wesley; Reading, MA, 1983; Part 2, pp 89-159.
(2) Collman, J. P.; Halbert, T. R.; Suslick, K. S. In *Metal Ion Activation of Dioxygen*; Spiro, T. G., Ed.; Wiley-Interscience, New York, 1980; pp 1-72.
(3) Watanabe, T.; Ama, T.; Nakamoto, K. *J. Phys. Chem.* **1984**, *88*, 440.
(4) Wagner, W.-D.; Paeng, I. R.; Nakamoto, K. *J. Am. Chem. Soc.* **1988**, *110*, 5565.
(5) Bajdor, K.; Nakamoto, K. *J. Am. Chem. Soc.* **1984**, *106*, 3045.
(6) Proniewicz, L. M.; Bajdor, K.; Nakamoto, K. *J. Phys. Chem.* **1986**, *90*, 1560.
(7) Chin, D.-H.; Del Gaudio, J.; La Mar, G. N.; Balch, A. L. *J. Am. Chem. Soc.* **1977**, *99*, 5486.
(8) Chin, D.-H.; La Mar, G. N.; Balch, A. L. *J. Am. Chem. Soc.* **1980**, *102*, 4344.
(9) Latos-Grazynski, L.; Cheng, R.-J.; La Mar, G. N.; Balch, A. L. *J. Am. Chem. Soc.* **1982**, *104*, 5992.

0002-7863/90/1512-3289$02.50/0

For example, ruthenium-substituted myoglobin[11] has been prepared and its reaction with carbon monoxide and dioxygen reported. Ruthenium-substituted horseradish peroxidase compound I (HRP-I)[12] has also been studied by NMR, ESR, and optical absorption spectroscopies.

In 1981 Collman et al.[13] reported that the pyrolysis of bis(pyridine)ruthenium(II) porphyrins produced binuclear ruthenium porphyrins containing a direct metal–metal double bond and that these unsaturated, binuclear complexes react with dioxygen to form stable oxo-bridged ruthenium(IV) porphyrin dimers possessing two axial hydroxy ligands. The hydroxy derivative of the μ-oxo dimer, (E) [see Scheme I, $((OEP)Ru(OH))_2O$ (OEP, octaethylporphyrin], has been isolated[13] and its crystal structure determined.[14] Groves et al.[15] and Dolphin et al.[16] prepared the dioxo complex, $Ru(TMP)(O)_2$ (D) (TMP, tetramesitylporphyrin) and assigned its $\nu_{as}(O{=}Ru{=}O)$ to the IR band at 821 cm^{-1}.[15] In this case, the sterically hindering methyl groups at the ortho positions of the meso-phenyl groups prevented the formation of the μ-oxo dimer. The monoxo ruthenium(IV) porphyrin, O=Ru(TMP) (C), has been produced by stoichiometric titration of $Ru(TMP)(O)_2$ with triphenylphosphine under anaerobic conditions, and the IR band at 823 cm^{-1} assigned[17] to its ν(RuO). Recently, Collman et al.[18] proposed a mechanism for irreversible oxidation of "base-free" ruthenium(II) porphyrins, which is similar to that for ferrous porphyrins.[7]

In the present work, we report the resonance Raman (RR) spectra of Ru(TPP) (TPP, tetraphenylporphyrin) analogues of B–D. All of these are produced in a toluene solution of Ru(TPP) saturated with dioxygen at low temperatures. At −80 °C, a toluene solution of Ru(TPP) produces the peroxo-bridged species, B, and monoxo species, C. When this solution is warmed to −40 °C, B and C are converted to the dioxo species, D, which is unique to ruthenium porphyrins. This dioxo complex can also be obtained by the reaction of Ru(TPP)CO or Ru(TMP)CO with *m*-chloroperoxybenzoic acid (*m*-CPBA). The vibrational (IR and RR) spectra of $Ru(TPP)(O)_2$ and $Ru(TMP)(O)_2$ thus obtained have been assigned by normal coordinate calculations on the O=Ru=O molecular fragment. We also obtained O=Ru(OEP), C, by saturating the solution of Ru(OEP) with dioxygen at low temperature. Although "base-bound", six-coordinate dioxygen adducts are well-known for Fe(II) complexes,[19] almost no information is available on the corresponding Ru(II) analogues.[20,21] In this work, we obtained the vibrational spectra of a six-coordinate dioxygen adduct, $Ru(TPP)(py)O_2$, for the first time. Finally, we report the RR spectra of intermediate species in the oxidation processes of Fe(TPP) and other Fe(II) porphyrins, which were not included in our previous paper.[22]

Experimental Section

Preparation of Compounds. $Ru(TPP)(py)_2$,[23] $Ru(OEP)(py)_2$,[23] $Fe(TPP)(pip)_2$,[24] and $Fe(OEP)(py)_2$[25] were prepared by the literature methods. Ru(TPP)(CO)MeOH, Ru(OEP)(CO)MeOH, Ru(TMP)(CO)MeOH, and H_2(TPP) were purchased from Midcentury, Posen, IL, and used without further purification. *m*-CPBA ($^{16}O_2$, $^{18}O_2$, and scrambled dioxygen) were prepared by the methods of Johnson[26] and Brown.[27] The solvents, toluene, toluene-d_8, and methylene chloride, and the bases, piperidine and pyridine, were purchased from Aldrich Chemical Co. Toluene and methylene chloride were dried by distillation from sodium metal and CaH_2, respectively. The gases, $^{16}O_2$ and $^{18}O_2$ (98.11%), were purchased from AIRCO Inc. and Monsanto Research, respectively, and used without further purification. Scrambled dioxygen was prepared by electrical discharge of an equimolar mixture of $^{16}O_2$ and $^{18}O_2$. Initially this gave a 1:2:1 mixture of $^{16}O_2/^{16}O^{18}O/^{18}O_2$, and more $^{16}O_2$ and $^{18}O_2$ were added until a 1:1:1 mixture was obtained. The mixing ratio of $^{16}O_2$, $^{16}O^{18}O$, and $^{18}O_2$ was determined by Raman spectroscopy.

Unligated iron(II) porphyrins were prepared by using either one of the following methods. First, iron(III) porphyrin dissolved in toluene was reduced to iron(II) porphyrin by zinc amalgam in a Dri-Lab HE/DL Series controlled atmosphere box under purified argon. Completion of the reduction was confirmed by UV–visible[28] and RR spectroscopy.[29] The solution was transferred to a minibulb,[30] which was attached to a vacuum stopcock. The sealed sample was removed from the glovebox and attached to a vacuum line and then the solution was degassed via five freeze–pump–thaw cycles. Alternatively, bis(pyridine)ruthenium(II) or bis(piperidine)iron(II) porphyrin (~0.2 mg) was heated in a minibulb at 220 °C for 5 h under high vacuum (1×10^{-4} Torr) to evaporate the base ligand. Next, the dry solvent, which was degassed by five freeze–pump–thaw cycles, was transferred via the vacuum line to the minibulb. The unligated metal(II) porphyrin solution thus obtained was immersed in a dry ice–acetone bath (−78 °C)[31] and left for ~20 min to attain equilibrium. Dioxygen gas was then introduced to the sample via the vacuum line and the minibulb was immersed in liquid nitrogen. The stem of the bulb was sealed and the minibulb stored in liquid nitrogen until it was attached to the front edge of a copper cold tip, which was cooled to ~70 K by a CTI Model 21 closed-cycle helium refrigerator.[30] The minibulb technique was also employed to measure the RR spectra of Ru(TPP)(CO), Ru(TMP)(CO), and their reaction products with *m*-CPBA and a six-coordinate oxygen adduct, $Ru(TPP)(py)O_2$.

Spectral Measurements. RR spectra were recorded on a Spex Model 1403 double monochromator coupled with a Spex DM1B data station and a Hamamatsu R-928 photomultiplier. Excitations were made by using Coherent Innova Model 100-K3 Kr-ion (406.7, 413.1, and 415.4 nm), Liconix He–Cd (441.6 nm), and Spectra-Physics 2025-05 Ar-ion (457.9 and 476.5 nm) lasers. The laser power on the sample was kept at 5–10 mW throughout this work. The sample temperature was calculated from the relative intensities of Stokes and anti-Stokes lines of the solvent. Calibration of the frequency reading was made by using the solvent bands. Estimated accuracy of frequency readings was ±1.0 cm^{-1}.

Results and Discussion

Oxidation of Ru(TPP)(CO) and Ru(TMP)(CO) with *m*-CPBA. Previously, Groves et al.[15,17] obtained $Ru(TMP)(O)_2$ as the final product of oxidation of Ru(TMP)CO with *m*-CPBA in methylene chloride and by aerobic oxidation of $Ru(TMP)(CH_3CN)_2$ in benzene-d_6. The IR band at 821 cm^{-1} was shifted to 785 cm^{-1} upon [$^{16}O/^{18}O$]-*m*-CPBA isotopic substitution and assigned to the $\nu_{as}(O{=}Ru{=}O)$ of this diamagnetic dioxo species. This compound was also characterized by using ^1H NMR and visible spectroscopy.[15]

We have prepared the dioxo complexes, $Ru(TPP)(O)_2$ via the oxidation of Ru(TPP)(CO) with *m*-CPBA containing $^{16}O_2$, $^{18}O_2$, and $^{16}O^{18}O$ peroxo bridges, and characterized them by using RR spectroscopy. Trace A of Figure 1 shows the RR spectrum (406.7-nm excitation) of $Ru(TPP)(O)_2$ obtained with ^{16}O-labeled *m*-CPBA in methylene chloride at −80 °C. This spectrum exhibits

(10) Balch, A. L.; Chan, Y.-W.; Cheng, R.-J.; La Mar, G. N.; Latos-Grazynski, L.; Renner, M. W. *J. Am. Chem. Soc.* **1984**, *106*, 7779.
(11) Paulson, D. R.; Addison, A. W.; Dolphin, D.; James, B. R. *J. Biol. Chem.* **1979**, *254*, 7002.
(12) Morishima, I.; Shiro, Y. Nakajima, K. *Biochemistry* **1986**, *25*, 3576.
(13) Collman, J. P.; Barnes, C. E.; Collins, T. J.; Brothers, P. J. *J. Am. Chem. Soc.* **1981**, *103*, 7030.
(14) Masuda, H.; Taga, T.; Osaki, K.; Sugimoto, H. Mori, M.; Ogoshi, H. *J. Am. Chem. Soc.* **1981**, *103*, 2199.
(15) Groves, J. T.; Quinn, R. *Inorg. Chem.* **1984**, *23*, 3844.
(16) Camenzind, M. J.; James, B. R.; Dolphin, D. *J. Chem. Soc., Chem. Commun.* **1986**, 1137.
(17) Groves, J. T.; Ahn, K.-H. *Inorg. Chem.* **1987**, *26*, 3831.
(18) Collman, J. P.; Brauman, J. I.; Fitzgerald, J. P.; Sparapany, J. W.; Ibers, J. A. *J. Am. Chem. Soc.* **1988**, *110*, 3486.
(19) Nakamoto, K.; Paeng, I. R.; Kuroi, T.; Isobe, T.; Oshio, H. *J. Mol. Struct.* **1988**, *189*, 293.
(20) Palson, D. R.; Bhakata, S. B.; Hyun, R. Y.; Yuen, M.; Beaird, C. E.; Lee, S. C.; Ybarra, J., Jr. *Inorg. Chim. Acta* **1988**, *151*, 149.
(21) Kim, D.; Su, Y. O.; Spiro, T. G. *Inorg. Chem.* **1986**, *25*, 3993.
(22) Paeng, I. R.; Shiwaku, H.; Nakamoto, K. *J. Am. Chem. Soc.* **1988**, *110*, 1995.
(23) Antipas, A.; Bucher, J. W.; Gouterman, M.; Smith, P. D. *J. Am. Chem. Soc.* **1987**, *100*, 3015.
(24) Epstein, L. M.; Straub, D. K.; Maricondi, C. *Inorg. Chem.* **1967**, *6*, 1720.
(25) Bonnet, R.; Dimsdale, M. J. *J. Chem. Soc., Perkin Trans. 2* **1972**, *1*, 2450.
(26) Johnson, R. A. *Tetrahedron Lett.* **1976**, *5*, 331.
(27) Brown, G. In *Organic Syntheses*; Wiley: New York, 1941; Collect. Vol. I, p 431.
(28) Gouterman, M. In *The Porphyrins*; Dolphin, D., Ed.; Academic Press: New York, 1978; Vol. IIIA, pp 1–165.
(29) Burke, J. M.; Kincaid, J. R.; Peters, S.; Gagne, R. R.; Collman, J. P.; Spiro, T. G. *J. Am. Chem. Soc.* **1978**, *100*, 6083.
(30) Nakamoto, K.; Nonaka, Y.; Ishiguro, T.; Urban, M. W.; Suzuki, M.; Kozuka, M.; Nishida, Y.; Kida, S. *J. Am. Chem. Soc.* **1982**, *104*, 3386.
(31) We also used a liquid bath instead of a dry ice bath and obtained the same results in both cases.

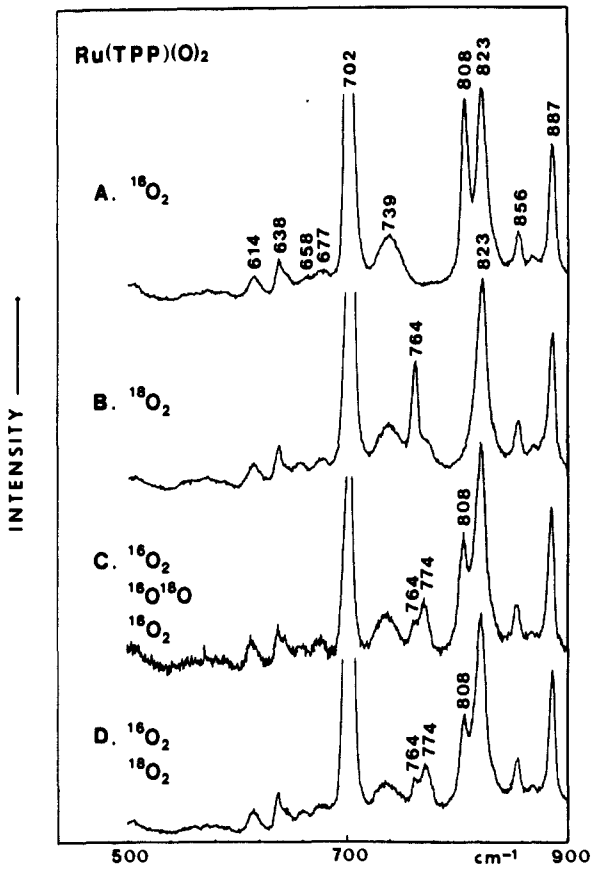

Figure 1. RR spectra (406.7-nm excitation) of $Ru(TPP)(O)_2$ obtained via the oxidation of Ru(TPP)(CO) with *m*-CPBA containing (A) $^{16}O^{16}O$, (B) $^{18}O^{18}O$, (C) scr-O_2 ($^{16}O^{16}O$:$^{16}O^{18}O$:$^{18}O^{18}O$ = 1:1:1), and (D) mixed O_2 ($^{16}O^{16}O$:$^{18}O^{18}O$ = 1:1), in methylene chloride at −80 °C.

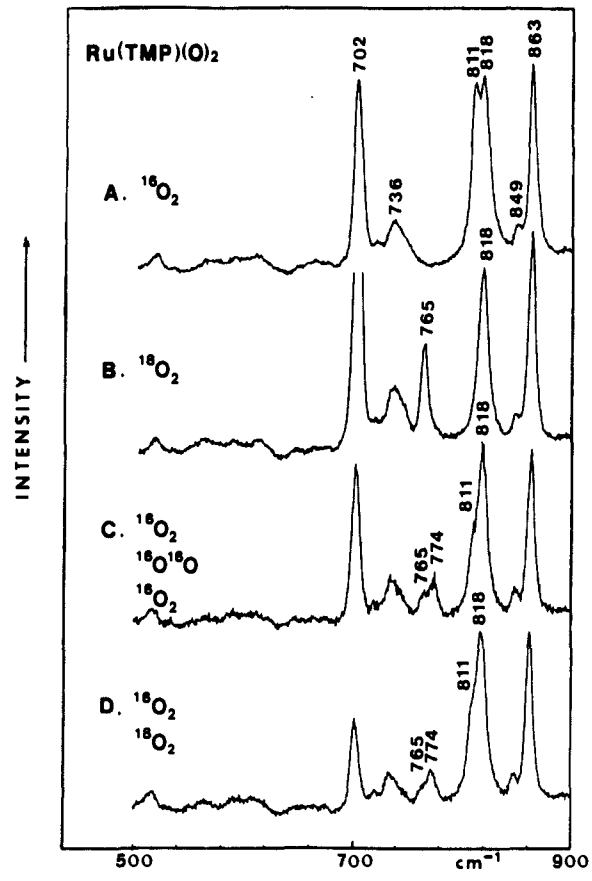

Figure 2. RR spectra (406.7-nm excitation) of $Ru(TMP)(O)_2$ obtained via the oxidation of Ru(TMP)(CO) with *m*-CPBA containing (A) $^{16}O^{16}O$, (B) $^{18}O^{18}O$, (C) scr-O_2, and (D) mixed O_2, in methylene chloride at −80 °C.

bands typical of Ru(TPP) at 823 and 887 cm^{-1} and a strong band at 808 cm^{-1}, which shifts to 764 cm^{-1} when ^{18}O-labeled *m*-CPBA is employed (trace B). A similar experiment with an isotopically scrambled oxidant (scr-*m*-CPBA, $^{16}O_2$:$^{16}O^{18}O$:$^{18}O_2$ = 1:1:1) gives three distinct Raman bands at 808, 774, and 764 cm^{-1} (trace C). It should be noted that the intensity pattern of these three peaks does not follow the mixing ratio of $^{16}O_2/^{16}O^{18}O/^{18}O_2$ in scr-*m*-CPBA used. Next, we oxidized Ru(TPP)(CO) with an equimolar mixture of the $^{16}O_2$- and $^{18}O_2$-labeled *m*-CPBA (mixed-*m*-CPBA) and obtained the RR spectrum shown in trace D. Even though no $^{16}O^{18}O$-labeled *m*-CPBA was present in this case, the spectrum showed the same intensity pattern as that of trace C. These oxygen-isotope-sensitive bands become weaker as the solution is warmed and disappear completely at room temperature.

Figure 2 shows the RR spectra of $Ru(TMP)(O)_2$ obtained by the oxidation of Ru(TMP)(CO) with *m*-CPBA containing $^{16}O_2$, $^{18}O_2$, and $^{16}O^{18}O$ peroxo bridges. The bands at 818 and 863 cm^{-1} are due to porphyrin skeletal modes of Ru(TMP). The strong band at 811 cm^{-1} (trace A) shifts to 765 cm^{-1} when $^{18}O_2$-labeled *m*-CPBA is used (trace B). Similar experiments with scr-*m*-CPBA (trace C) and mixed-*m*-CPBA (trace D) yield three oxygen-isotope-sensitive bands at 811, 774, and 765 cm^{-1}, which remain for several hours even at room temperature. These results indicate that $Ru(TMP)(O)_2$ is much more stable than $Ru(TPP)(O)_2$ since the dioxo group of the former is protected by the mesityl groups around the porphyrin core. In fact, $Ru(TMP)(O)_2$ can be isolated as crystals and its IR spectrum measured at room temperature as shown in Figure 3. Traces A and B are the IR spectra of $Ru(TMP)(O)_2$ obtained by using ^{16}O-labeled *m*-CPBA and ^{18}O-labeled *m*-CPBA, respectively. It is seen that the strong band at 821 cm^{-1} (trace A) is shifted to 785 cm^{-1} (trace B) by [$^{16}O/^{18}O$]-*m*-CPBA isotope substitution. These spectra are in good agreement with that obtained by Groves and Quinn.[15] Trace C shows the IR spectrum of $Ru(TMP)(O)_2$, which was obtained by using scr-*m*-CPBA ($^{16}O_2$:$^{16}O^{18}O$:$^{18}O_2$ = 1:1:1). It shows four

Table I. Observed and Calculated Frequencies of Dioxoruthenium(VI) Porphyrin Complexes[a]

		$\nu_s(\nu_1)$, cm^{-1}		$\nu_{as}(\nu_3)$, cm^{-1}	
		obs	calc	obs	calc
TMP	$^{16}ORu^{16}O$	811 (R)	811	821 (IR)	821
	$^{16}ORu^{18}O$	774 (R)	774	816 (IR)	817
		777 (IR)		(R)	
	$^{18}ORu^{18}O$	765 (R)	765	785 (IR)	786
TPP	$^{16}ORu^{16}O$	808 (R)	811		
	$^{16}ORu^{18}O$	774 (R)	774		
	$^{18}ORu^{18}O$	764 (R)	765		

[a] Force constants: K(O=Ru=O), 5.54 mdyn/Å; K'(interaction), 0.69 mdyn/Å.

oxygen-isotope-sensitive bands at 821, 816, 785, and 777 cm^{-1}, as expected for a mixture of the three linear moieties, (^{16}O)Ru(^{16}O), (^{16}O)Ru(^{18}O), and (^{18}O)Ru(^{18}O) [see below (Table I)].

Normal Coordinate Calculation. In order to assign the oxygen-isotope-sensitive bands, normal coordinate calculations were carried out on the linear O=Ru=O moiety. In a linear XY_2-type molecule ($^{16}ORu^{16}O$, $^{18}ORu^{18}O$), the ν_s(O=Ru=O) is Raman active but not IR active, whereas ν_{as}(O=Ru=O) is IR active but not Raman active (mutual exclusion rule). However, both vibrations are IR as well as Raman active in a linear XYZ-type molecule (^{16}O=Ru=^{18}O).

The stretching frequencies (ν_1 and ν_3) of a linear XYZ-type molecule (^{16}O=Ru=^{18}O) are given by[32]

$$4\pi^2(\nu_1^2 + \nu_3^2) = K_{xy}/M_x + K_{yz}/M_z + (K_{xy} + K_{yz} - 2K')/M_y$$

$$16\pi^4\nu_1^2\nu_3^2 = [K_{xy}K_{yz} - (K')^2]\,(M_x + M_y + M_z)/M_xM_yM_z$$

Here, K_{xy} and K_{yz} are the stretching force constants of the X–Y

(32) Maki, A.; Decius, J. C. *J. Chem. Phys.* **1959**, *31*, 772.

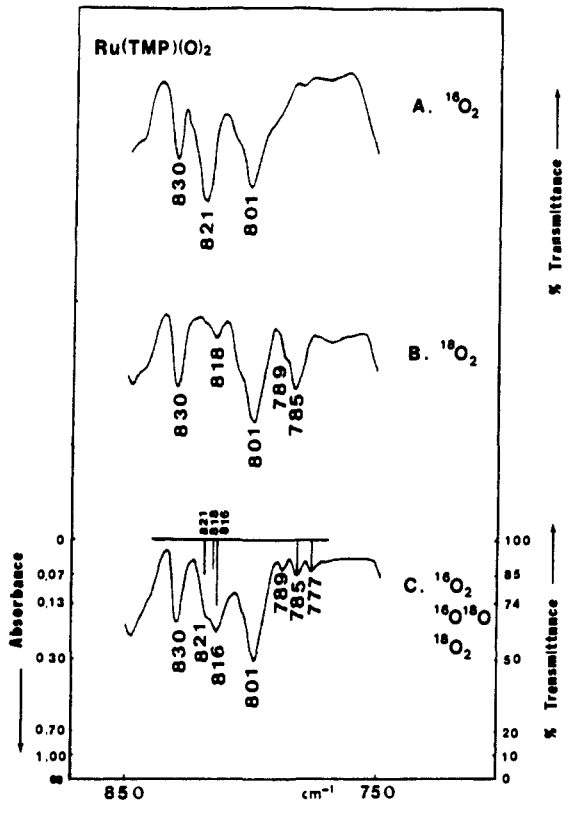

Figure 3. IR spectra of $Ru(TMP)(O)_2$ obtained via the oxidation of Ru(TMP)(CO) with *m*-CPBA containing (A) $^{16}O^{16}O$, (B) $^{18}O^{18}O$, and (C) scr-O_2.

and Y–Z bonds, respectively, and K' is an interaction force constant between the X–Y and Y–Z stretching vibrations. M_x, M_y, and M_x are the masses of X, Y, and Z atoms, respectively. A linear XYX-type molecule ($^{16}O{=}Ru{=}^{16}O$ and $^{18}O{=}Ru{=}^{18}O$) is regarded as a special case where $M_x = M_z$, $K_{xy} = K_{yz} = K$. Using K = 5.54 mdyn/Å and K' = 0.69 mdyn/Å, we calculated the O=Ru=O stretching frequencies of the three dioxo moieties. As seen in Table I, the agreement between the observed and calculated frequencies is excellent. It is of particular interest to compare the ν_1 and ν_3 frequencies of $^{16}O{=}Ru{=}^{18}O$ with those of $^{16}O{=}Ru{=}^{16}O$ and $^{18}O{=}Ru{=}^{18}O$. The ν_1 frequency of $^{16}O{=}Ru{=}^{18}O$ [774 (R), 777 (IR) cm^{-1}] is not the average of the corresponding frequencies for $^{16}O{=}Ru{=}^{16}O$ (811 cm^{-1}) and $^{18}O{=}Ru{=}^{18}O$ (765 cm^{-1}). Similarly, the ν_3 frequency of $^{16}O{=}Ru{=}^{18}O$ (816 cm^{-1}) is not the average of the corresponding frequencies for $^{16}O{=}Ru{=}^{16}O$ (821 cm^{-1}) and $^{18}O{=}Ru{=}^{18}O$ (785 cm^{-1}). The ν_3 and ν_1 of $^{16}O{=}Ru{=}^{18}O$ are close to $\nu_{as}(^{16}O{=}Ru{=}^{16}O)$ and $\nu_s(^{18}O{=}Ru{=}^{18}O)$, respectively, since in a linear XYZ-type molecule,[33] ν_3 is largely due to $\nu(Ru{=}^{16}O)$ whereas ν_1 is mainly due to $\nu(Ru{=}^{18}O)$.

Reaction Mechanism of Oxidation with *m*-CPBA. As seen in Figures 1 and 2, the ν_1 of $^{16}O{=}Ru{=}^{18}O$ at 774 cm^{-1} is ~2 times stronger than the ν_s of $^{18}O{=}Ru{=}^{18}O$ at 765 cm^{-1}. In the IR spectra shown in Figure 3, the ν_3 of $^{16}O{=}Ru{=}^{18}O$ at 816 cm^{-1} is much stronger than the ν_{as} of $^{18}O{=}Ru{=}^{18}O$ at 785 cm^{-1}. Furthermore, we found that the same intensity patterns are obtained regardless of the mixing ratio of the $^{16}O_2$-, $^{16}O^{18}O$-, and $^{18}O_2$-labeled derivatives in scr-*m*-CPBA (1:2:1, 1:1:1, and 1:0:1, etc.) as long as the total concentrations of ^{16}O and ^{18}O in the mixture are the same (vide infra). These observations can be accounted for by assuming the reaction Scheme II.

First, the labeled ^{a}O–^{b}O bond is cleaved in going from II to III. Since the leaving group competes with the second *m*-CPBA, which is more reactive than the leaving group, the latter attacks the vacant axial site on the ruthenium porphyrin (IV), resulting

Scheme II

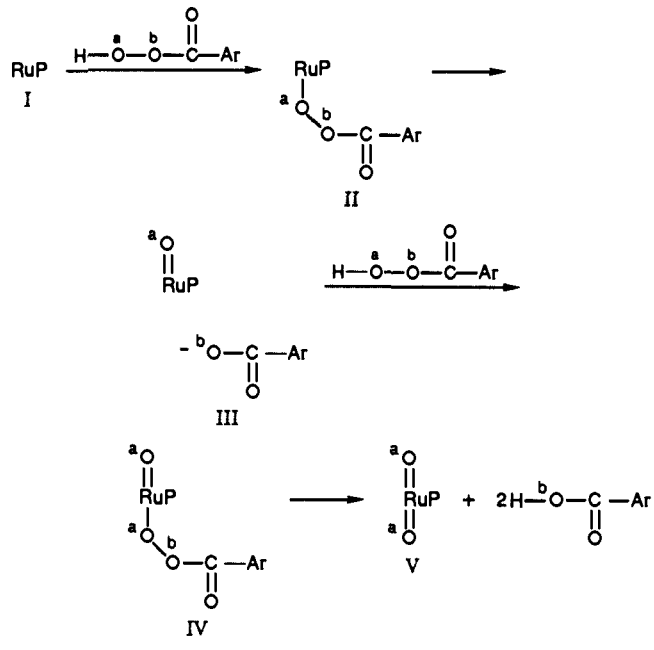

in the formation of the final dioxo complex (V). Thus, this reaction requires 2 equiv of *m*-CPBA. A clear isosbestic point has been observed in visible spectra[15] since the life times of the reaction intermediates II–IV are extremely short. The step I–II is the same as that proposed by Groves and Watanabe[34] for the oxidation of Fe(TMP)(OH) with several oxidants including *m*-CPBA. As shown above, the dioxo species, $Ru(TMP)(O)_2$ and $Ru(TPP)(O)_2$, are formed via successive O–O bond cleavage of the oxidant at low temperature. It should be pointed out, however, that the oxidation of ruthenium porphyrin with *m*-CPBA is different from that of iron porphyrin; in the former, the metal center is reoxidized to form a six-coordinate dioxo species while, in the latter, the porphyrin ring is oxidized to form a five-coordinate π cation radical,[34,35] $O{=}FeP^{\bullet+}$, which exhibits the ν(Fe=O) at 802 cm^{-1} (767 cm^{-1} for the ^{18}O analogue).[35]

Next we consider the concentration ratio of the isotopic dioxo species in the final product. In our experiments, we employed four different oxygen-labeled *m*-CPBA, which contained H–$\underline{^{16}O}$–^{16}O–/H–$\underline{^{16}O}$–^{18}O–/H–$\underline{^{18}O}$–^{16}O–/H–$\underline{^{18}O}$–^{18}O–C(O)–Ar (Ar = *m*-ClC_6H_4), in a ratio of 1:*x*:*x*:1 (x = 0 for 1:0:1, x = 1/2 for 1:1:1, and x = 1 for 1:2:1) (scr-*m*-CPBA). We can regard H–$\underline{^{16}O}$–^{16}O– and H–$\underline{^{16}O}$–^{18}O– as the same oxidant since only the oxygen bonded to the hydrogen (^{a}O) would bind to the ruthenium to yield the $^{a}O{=}Ru$ bond (III). Similarly, H–$\underline{^{18}O}$–^{16}O– and H–$\underline{^{18}O}$–^{18}O– are regarded as the same oxidant. Thus, the ratio of the $^{16}O{=}Ru/^{18}O{=}Ru$ formed is (1 + x):(1 + x); i.e., 1:1, regardless of the mixing ratio of [$^{16}O_2$/$^{16}O^{18}O$($^{18}O^{16}O$)/$^{18}O_2$]-*m*-CPBA. Since the same ratio holds for the second oxygen-labeled *m*-CPBA, the ratio of the final products ($^{16}O{=}Ru{=}^{16}O$, $^{16}O{=}Ru{=}^{18}O$, $^{18}O{=}Ru{=}^{16}O$, and $^{18}O{=}Ru{=}^{18}O$) should be 1:1:1:1. Namely, the ratio of the dioxo species is always 1:2:1. Trace C of Figure 3 also shows the IR intensity on the absorbance scale, which is proportional to the concentration. As expected, the intensity ratio of the three bands at 821, 816, and 785 cm^{-1} is 1:2:1. The band at 821 cm^{-1} appears stronger than expected from the 1:2:1 ratio since it is partially overlapped by the TMP band at 818 cm^{-1}. The IR intensities of the bands at 816 (ν_3), and 777 cm^{-1} (ν_1) of $\nu(^{16}O{=}Ru{=}^{18}O)$ are not equal since the asymmetric stretching character of the former makes it stronger than the latter.

Oxidation of Ru(TPP) with Dioxygen. The RR spectra of a dry, degassed solution of "base-free" Ru(TPP) saturated with

(33) Herzberg, G. In *Infrared and Raman Spectra of Polyatomic Molecules*; D. Van Nostrand Co., Inc.: New York, 1945; p 174.

(34) Groves, J. T.; Watanabe, Y. *J. Am. Chem. Soc.* **1986**, *108*, 7834.
(35) Kincaid, J. R.; Schneider, A. J.; Paeng, K.-J. *J. Am. Chem. Soc.* **1989**, *111*, 735.

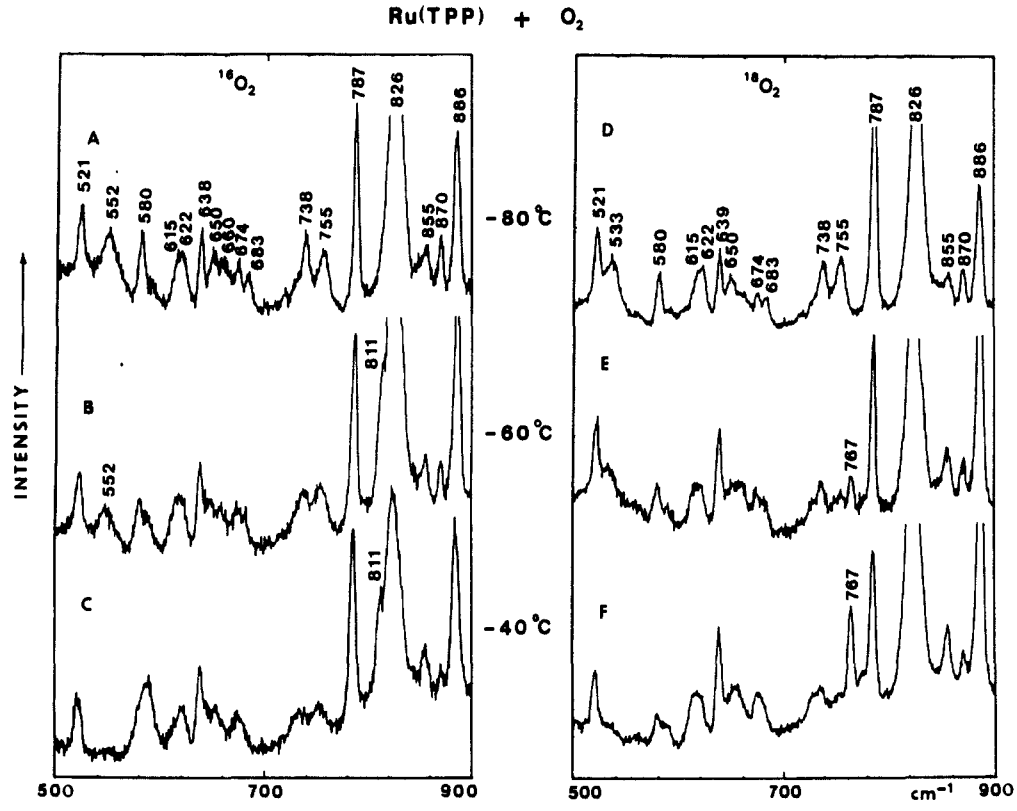

Figure 4. RR spectra (406.7-nm excitation) of Ru(TPP) in toluene, which were saturated with O_2. (A) $^{16}O_2$, −80 °C; (B) $^{16}O_2$, −60 °C; (C) $^{16}O_2$, −40 °C; (D) $^{18}O_2$, −80 °C; (E) $^{18}O_2$, −60 °C; (F) $^{18}O_2$, −40 °C.

dioxygen were measured at three different temperatures. Trace A of Figure 4 shows the RR spectrum of Ru(TPP) in toluene saturated with $^{16}O_2$ at −80 °C. The bands typical of Ru(TPP) are at 826 and 886 cm^{-1}. These frequencies are 3 cm^{-1} higher and 1 cm^{-1} lower, respectively, than those obtained in CH_2Cl_2 solution (Figure 1). At −80 °C, a band appears at 552 cm^{-1}. When the solution is warmed to −60 °C (trace B), this band becomes weaker and a new band appears at 811 cm^{-1} as a shoulder on the porphyrin band at 826 cm^{-1}. At −40 °C (trace C), the former disappears completely and the latter becomes stronger relative to the TPP band at 826 cm^{-1}. The same trend is observed in a series of the spectra obtained with $^{18}O_2$ (traces D–F); at −80 °C, the band corresponding to the 552-cm^{-1} band of trace A appears at 533 cm^{-1} (trace D). At −60 °C, this band loses its intensity and a new band corresponding to the 811-cm^{-1} band of trace B appears at 767 cm^{-1} (trace E). At −40 °C, the 533-cm^{-1} band disappears while the 767-cm^{-1} feature becomes stronger (trace F). To examine the nature of these bands, we continued our study with scrambled dioxygen.

Trace A of Figure 5 shows the RR spectrum of a toluene solution of Ru(TPP) saturated with scrambled oxygen ($^{16}O_2$:^{16}O-^{18}O;$^{18}O_2$ = 1:1:1) at −80 °C. It exhibits two oxygen-isotope-sensitive bands of equal intensity at 552 and 533 cm^{-1}, which can be assigned to the ν_s(Ru–^{16}O) and ν_s(Ru–^{18}O) of the peroxo-bridged species (B), (TPP)Ru–^{16}O–^{16}O–Ru(TPP), and its $^{18}O_2$ analogue, respectively. This assignment is based on the following observations: (1) These bands cannot be attributed to the ν(Ru–O) of Ru(TPP)O_2 since such a "base-free" O_2 adduct is expected to be stable only in O_2 matrices[4,36] and rapidly oxidized to form (TPP)Ru–O–O–Ru(TPP) in toluene solution.[22] Furthermore, the observed $^{16}O_2/^{18}O_2$ isotopic shift ($\Delta\nu$ = 19 cm^{-1}) is much smaller than that expected for the Ru–O diatomic vibrator ($\Delta\nu$ = 27 cm^{-1}). (2) These bands cannot be assigned to the ν(Ru–O) of a six-coordinate dioxygen adduct, Ru(TPP)(py)O_2, which might have been produced from a Ru(TPP)$(py)_2$ impurity. As will be shown later, this band is observed at 603 cm^{-1} for $^{16}O_2$ (574 cm^{-1} for $^{18}O_2$) in toluene solution. (3) These bands cannot be assigned to the ν_s(Ru–O–Ru) of the μ-oxo-type dimer since

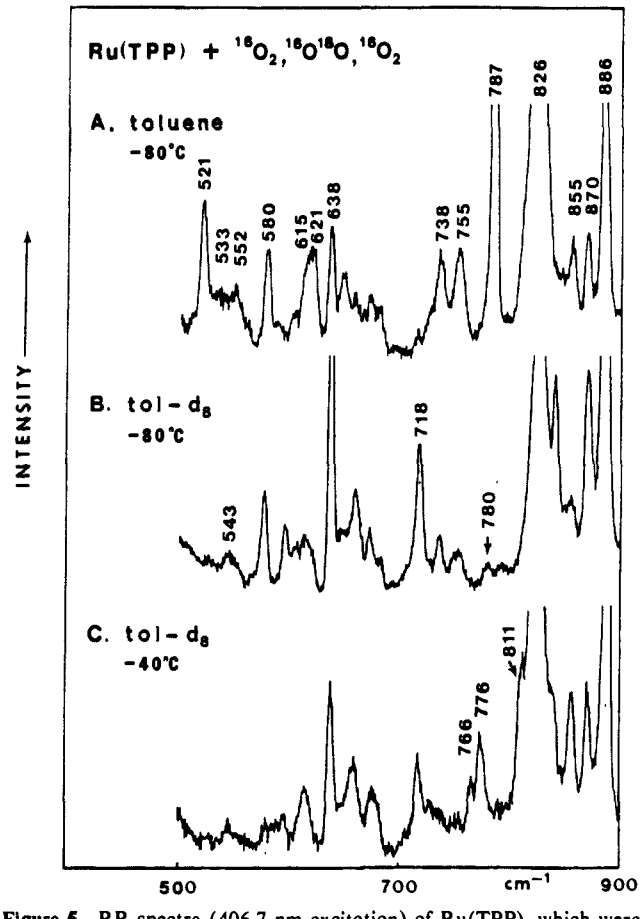

Figure 5. RR spectra (406.7-nm excitation) of Ru(TPP), which were saturated with scr-O_2 ($^{16}O_2$:$^{16}O^{18}O$:$^{18}O_2$ = 1:1:1) in (A) toluene, −80 °C; (B) toluene-d_8, −80 °C; and (C) toluene-d_8, −40 °C.

(36) Lewandowski, W.; Paeng, I. R.; Proniewicz, L. M.; Nakamoto, K., in preparation.

such a vibration should appear near 366 cm^{-1} where the ν_s(Fe–O–Fe) of the μ-oxo dimer, (TPP)Fe–O–Fe(TPP), is observed.[37]

As seen in trace C of Figure 4, a new band appears at 811 cm^{-1} at −40 °C, which is shifted to 767 cm^{-1} by $^{16}O_2/^{18}O_2$ substitution (trace F). In order to determine whether this band is the ν(RuO) of the monoxo or the ν_s(O=Ru=O) of the dioxo species of Ru(TPP), similar experiments were carried out with scrambled dioxygen using toluene-d_8 as the solvent. The resulting spectrum at −80 °C (trace B of Figure 5) shows that the toluene band at 787 cm^{-1} is shifted to 718 cm^{-1} in toluene-d_8, and that the two bands at 552 ($^{16}O_2$) and 533 cm^{-1} ($^{18}O_2$) observed in toluene solution are now obscured by the broad toluene-d_8 band at 543 cm^{-1}. Upon warming the solution to −40 °C (trace C), however, three new bands emerge at 766, 776, and 811 cm^{-1}, which completely disappear at room temperature. These three bands cannot be attributed to the ν(RuO) of the monoxo species, O=Ru(TPP), since only two bands are expected for the isotopically scrambled monoxo species. Furthermore, these bands cannot be assigned to the $\nu(O_2)$ of the peroxo-bridged species (B) since such a species is expected to be unstable at −40 °C. Finally, the intensity ratio of these three bands does not match the concentration ratio of the isotopic dioxygens used (1:1:1); the middle band at 776 cm^{-1} is ~2 times stronger than the band at 766 cm^{-1}. In fact, these peaks show exactly the same intensity pattern as that of Ru(TPP)$(O)_2$, which was obtained previously via the reaction of Ru(TPP)CO with *m*-CPBA (Figure 1). Thus we assign these bands to the ν_s(O=Ru=O) of the dioxo species. The slight frequency shifts observed are attributable to the different solvents used in these experiments (CH_2Cl_2 vs toluene-d_8).

We assign a weak band at 780 cm^{-1} in trace B of Figure 5 to the $\nu(Ru^{18}O)$ of O=Ru(TPP) (C). Although the corresponding $\nu(Ru^{16}O)$ band is not seen in trace A, it is probably hidden under the TPP band at 826 cm^{-1} since an upward shift of 40 cm^{-1} is expected by $^{16}O/^{18}O$ isotopic substitution. We also prepared ^{16}O=Ru(TPP-d_8) to observe this vibration. However, the region between 750 and 850 cm^{-1} was still obscured by two strong TPP-d_8 bands at 809 and 777 cm^{-1}, which were shifted from 826 and 1079 cm^{-1}, respectively, by the deuteriation of TPP. As will be shown later, the $\nu(Ru^{16}O)$ of the monoxo complex was clearly observed at 820 cm^{-1} in the case of Ru(OEP).

The results described above suggest the following oxidation process:

$$\underset{A}{Ru(TPP)} + O_2 \rightarrow \underset{B}{(TPP)RuOORu(TPP)} \rightarrow \underset{C}{(TPP)RuO} \rightarrow \underset{D}{Ru(TPP)(O)_2}$$

At −80 °C, the unligated porphyrin (A) is oxidized to yield the peroxo-bridged species (B), which is in equilibrium with the monoxo species (C). Upon warming to −40 °C, the latter turns to the dioxo species (D). This process is slightly different from that suggested by Collman et al.[18] (vide supra) in that, in a dry toluene solution, the dioxo species is formed instead of the hydroxy μ-oxo dimer even for Ru(TPP). The fact that the ν_s(Ru—O) of the peroxo-bridged species, the ν(RuO) of the monoxo species and the ν_s(O=Ru=O) of the dioxo species were observed only by excitation in the 406–415-nm region suggests that all these modes are vibronically coupled with the Soret π–π^* transition.

Oxidation of Ru(OEP) with Dioxygen. Traces A and B of Figure 6 show the RR spectra of Ru(OEP) in toluene-d_8, which was saturated with $^{16}O_2$ and $^{18}O_2$, respectively, at −80 °C. It is seen that a weak band at 820 cm^{-1} (trace A) is shifted to 779 cm^{-1} by $^{16}O_2/^{18}O_2$ substitution (trace B). The observed isotopic shift ($\Delta\nu$ = 41 cm^{-1}) is in good agreement with the calculated value ($\Delta\nu$ = 40 cm^{-1}) for a diatomic Ru=O vibrator. Thus, we assign the bands at 820 and 779 cm^{-1} to the $\nu(Ru^{16}O)$ and $\nu(Ru^{18}O)$ of the monoxo species, respectively. Similar experiments with a scrambled dioxygen ($^{16}O_2$:$^{16}O^{18}O$:$^{18}O_2$ = 1:1:1) gave two bands at 820 and 779 cm^{-1} (trace C), thus confirming our assignments.

(37) Burke, J. M.; Kincaid, J. R.; Spiro, T. G. *J. Am. Chem. Soc.* **1978**, *100*, 6077.

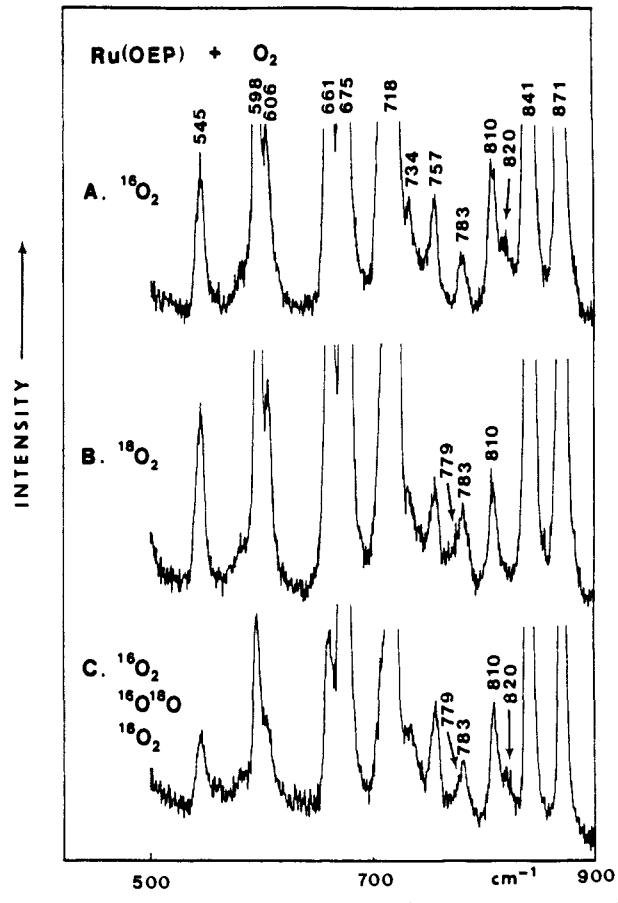

Figure 6. RR spectra (406.7-nm excitation) of Ru(OEP) in toluene-d_8, which were saturated with O_2 at −80 °C. (A) $^{16}O_2$, (B) $^{18}O_2$, (C) scr-O_2.

Table II. Comparison of Oxygen Adducts of Fe(II)(TPP) and Ru(II)(TPP)[d]

	ν(M–O)	$\nu(O_2)$	ref
Fe(TPP)(pip)O_2	575 (551)	1157 (1093)	1
Ru(TPP)(py)O_2	603 (574)	1103 (1041)[b]	*a*
Fe(TPP)O_2	509 (487)	1195 (1129)	4
Ru(TPP)O_2		1167 (1107)[c]	*a*
O=Fe(TPP)	845 (812)		*a*
O=Ru(TPP)	820 (780)		*a*
[Fe(TPP)]$_2O_2$	577 (553)		*a*
[Ru(TPP)]$_2O_2$	552 (533)		*a*

[a] This work. [b] Reference 18. [c] Reference 36. [d] The number in parentheses indicates the frequency of the ^{18}O species.

Recently, Groves and Ahn[17] measured the IR spectrum of O=Ru(TMP) via stoichiometric titration of Ru(TMP)$(O)_2$ with triphenylphosphine under anaerobic conditions and assigned the bands at 823 and 782 cm^{-1} to the $\nu(Ru^{16}O)$ and $\nu(Ru^{18}O)$ of the monoxo complex, respectively. Small differences in frequency (3 cm^{-1}) between our RR and their IR frequencies[17] may be attributed to the difference in the medium used. It should be noted that the oxidation of Ru(OEP) under the same conditions as that used for Ru(TPP) produces only the monoxo species; the peroxo-bridged species is unstable even at −80 °C. Bands assignable to the dioxo (~810 cm^{-1}) and/or hydroxy μ-oxo species (~360 cm^{-1})[37] were not observed upon warming, probably because these vibrations were not enhanced by the excitation at the 406-nm line of an Kr-ion laser, which is too far from its Soret band at 376 nm.

Oxidation of Ru(TPP)$(py)_2$ with Dioxygen. Traces A–C of Figure 7 show the low-frequency RR spectra of six-coordinate dioxygen adducts, Ru(TPP)(py)O_2, which were obtained by saturating the toluene solution of Ru(TPP)$(py)_2$ with $^{16}O_2$, $^{18}O_2$, and scrambled dioxygen (1:1:1), respectively, at −80 °C. The band at 603 cm^{-1} (trace A) is shifted to 574 cm^{-1} by $^{16}O_2/^{18}O_2$ isotopic

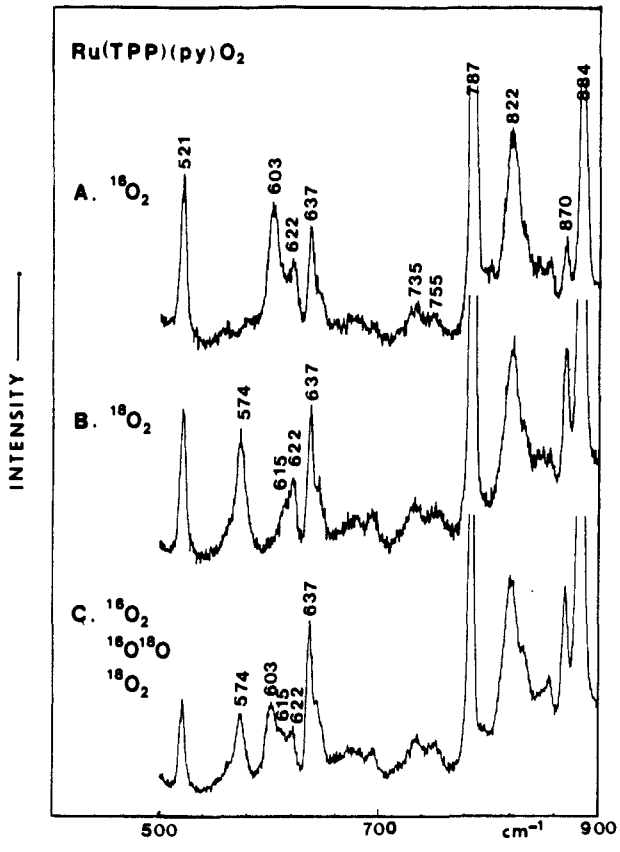

Figure 7. RR spectra (406.7-nm excitation) of Ru(TPP)(py)O_2 in toluene at −80 °C. (A) $^{16}O_2$, (B) $^{18}O_2$, (C) scr-O_2.

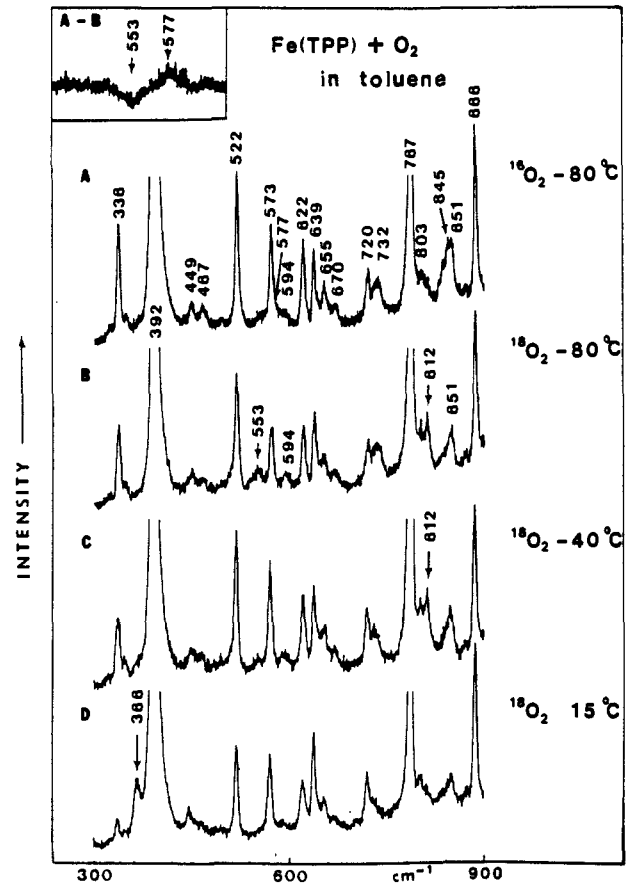

Figure 8. RR spectra (low-frequency region) of the Fe(TPP) in toluene, which were saturated with O_2. (A) $^{16}O_2$, −80 °C; (B) $^{18}O_2$, −80 °C; (C) $^{18}O_2$, −40 °C; (D) $^{18}O_2$, 15 °C.

substitution (trace B). Furthermore, the scrambled dioxygen solution (trace C) exhibits two bands at 603 and 574 cm^{-1}. The observed shift ($\Delta\nu$ = 29 cm^{-1}) is in perfect agreement with the theoretical value ($\Delta\nu$ = 29 cm^{-1}) expected for a diatomic Ru–O vibrator. Thus, the bands at 603 and 574 cm^{-1} are assigned to the ν(Ru–O) of Ru(TPP)(py)O_2 and its $^{18}O_2$ analogue, respectively. Table II compares $\nu(O_2)$ and ν(M–O) of various oxygen adducts of Ru(TPP) with those of corresponding Fe(TPP) complexes. The ν(Ru–O) of Ru(TPP)(py)O_2 (603 cm^{-1}) is higher than the ν(Fe–O) of Fe(TPP)(pip)O_2 (575 cm^{-1}).[19] On the other hand, the $\nu(O_2)$ of Ru(C6-PBP)(1,5-DCI)O_2 (PBP, picnic-basket porphyrin; 1,5-DCI, 1,5-dicyclohexylimidazole) (1103 cm^{-1})[18] is lower than that of Fe(TPP)(pip)O_2 (1157 cm^{-1}).[19] The same trend is seen in the $\nu(O_2)$ between Ru(TPP)O_2 (1167 cm^{-1})[36] and Fe(TPP)O_2 (1195 cm^{-1}).[4] Since the Ru 4d orbital is extended further than the Fe 3d orbital, π back-donation[21] from the metal to dioxygen is expected to be more effective in Ru than in Fe. This would decrease the $\nu(O_2)$ and increase the ν(M–O) in Ru porphyrins relative to Fe porphyrins. Although the ν(RuO) of O=Ru(TPP) and ν_s(Ru—O) of [Ru(TPP)]$_2O_2$ are lower than those of the corresponding Fe analogues, these frequencies still demonstrate the presence of the stronger π back-donation in the Ru than in the Fe complexes; if there were only mass effect, the ν(RuO) of these complexes would be 802 and 547 cm^{-1}, respectively, which are lower than those observed (Table II).

Oxidation of Fe(TPP) with Dioxygen. In the previous communication,[22] we reported the RR spectra of toluene solution of Fe(TMP) saturated with dioxygen, which contained a mixture of the peroxo-bridged dimer, (TMP)Fe–O–O–Fe(TMP), and ferryltetramesitylporphyrin, (TMP)Fe=O. In this work, we carried out similar experiments with Fe(TPP) including the high-frequency region. Traces A and B of Figure 8 show the RR spectra of toluene solutions of Fe(TPP) saturated with the $^{16}O_2$ and $^{18}O_2$, respectively, at ~−80 °C. It is seen that the band at 577 cm^{-1} shifts to 553 cm^{-1} (trace B) by $^{16}O_2/^{18}O_2$ isotopic substitution. Although the former band is obscured by the strong 573-cm^{-1} band, its presence can be confirmed by subtraction of trace B from trace A as shown in the inset. Previously, the band observed at 574 cm^{-1} was assigned to the ν_s(Fe–O) of (TMP)-Fe–O–O–Fe(TMP).[22] Thus, it is reasonable to assign the bands at 577 and 553 cm^{-1} to the ν_s(Fe–O) of the peroxo-bridged species, (TPP)Fe–^{16}O–^{16}O–Fe(TPP) and its ^{18}O–^{18}O analogue, respectively. The band at 845 cm^{-1} (trace A) is also shifted to 812 cm^{-1} (trace B) by $^{16}O_2/^{18}O_2$ isotopic substitution. As shown previously, these bands can be assigned to the ν(FeO) of ^{16}O=Fe(TPP) and its ^{18}O analogue, respectively, which are characteristic of five-coordinate ferryl porphyrins.[4,5,6,22,38] Traces B–D of Figure 8 show a series of spectral changes observed by raising the temperature of the toluene solution of Fe(TPP) oxidized with $^{18}O_2$. As mentioned above, trace B represents a mixture of the peroxo-bridged dimer and the ferryl species. At −40 °C, the former is converted to O=Fe(TPP) (trace C). When the solution is warmed to 15 °C (trace D), both bands at 553 and 812 cm^{-1} disappear completely and a new band appears at 366 cm^{-1}. The latter band shows no shift by $^{16}O_2/^{18}O_2$ isotopic substitution, and has already been assigned to the ν_s(FeOFe) of the μ-oxo dimer, (TPP)Fe–O–Fe(TPP).[37]

Figure 9 shows a series of spectral changes obtained for a toluene solution of Fe(TPP) saturated with O_2 in the high-frequency region. Traces A–E were obtained at ~−80, ~−60, ~−40, ~−20, and ~15 °C, respectively. Recently, Spiro et al.[39] and Chottard et al.[40] noted that FeTPP(L)(L′)-type complexes have several structure-sensitive bands, which reflect the oxidation and spin states of the Fe center; the band at ~1560 cm^{-1} (ν_2, p) is

(38) Hashimoto, S.; Tatsuno, Y.; Kitagawa, T. In *Proceedings of the Tenth International Conference on Raman Spectroscopy*; Peticolas, W. L., Hudson, B., Eds.; University of Oregon: Eugene, OR, 1986; pp 1–28.
(39) Stong, J. D.; Spiro, T. G.; Kubaska, R. J.; Shupack, S. I. *J. Raman Spectrosc.* **1980**, *9*, 312.
(40) Chottard, G.; Battioni, P.; Battioni, J.-P.; Lange, M.; Mansuy, D. *Inorg. Chem.* **1982**, *20*, 1718.
(41) Bajdor, K.; Oshio, H.; Nakamoto, K. *J. Am. Chem. Soc.* **1984**, *106*, 7273.

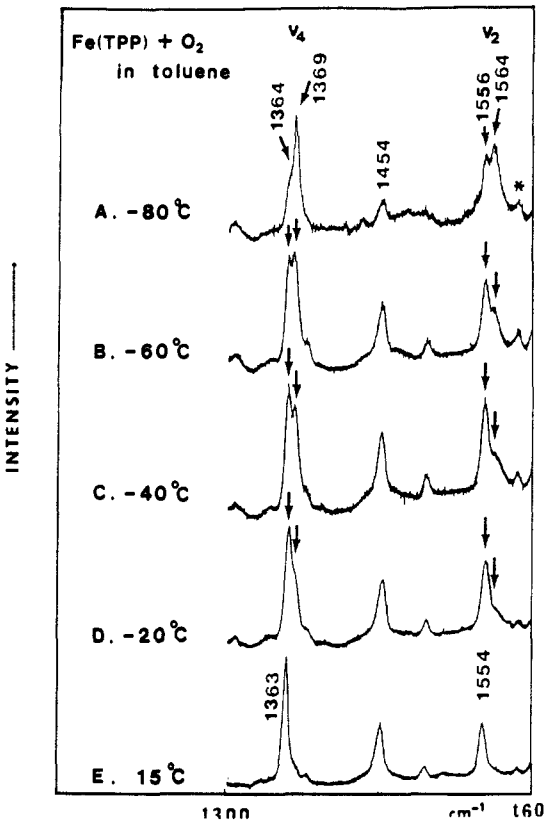

Figure 9. RR spectra (high-frequency region) of the Fe(TPP) in toluene, which were saturated with $^{18}O_2$ at (A) -80, (B) -60, (C) -40, (D) -20, and (E) 15 °C.

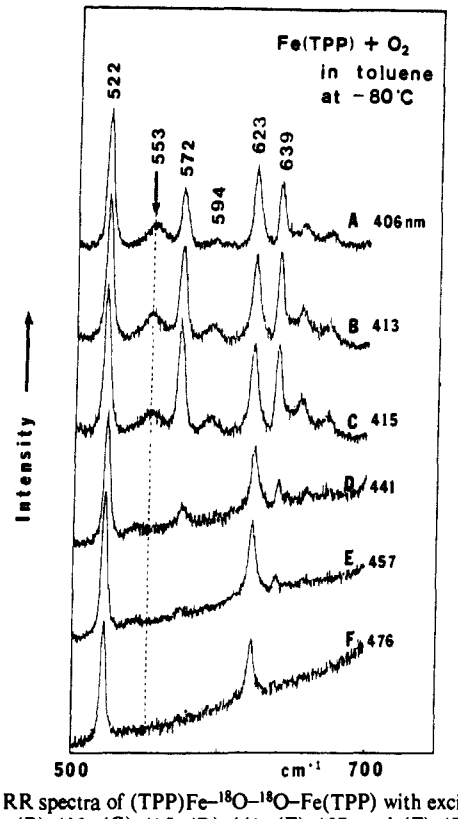

Figure 10. RR spectra of (TPP)Fe-^{18}O-^{18}O-Fe(TPP) with exciting lines at (A) 406, (B) 413, (C) 415, (D) 441, (E) 457, and (F) 476 nm, in toluene at -80 °C.

mainly spin-state sensitive and the band at ~1360 cm^{-1} (ν_4, p) is sensitive to both oxidation and spin state. At -80 °C, the solution consists of a mixture of the peroxo-bridged dimer and the ferryl species. There are two pairs of ν_4 and ν_2 that are

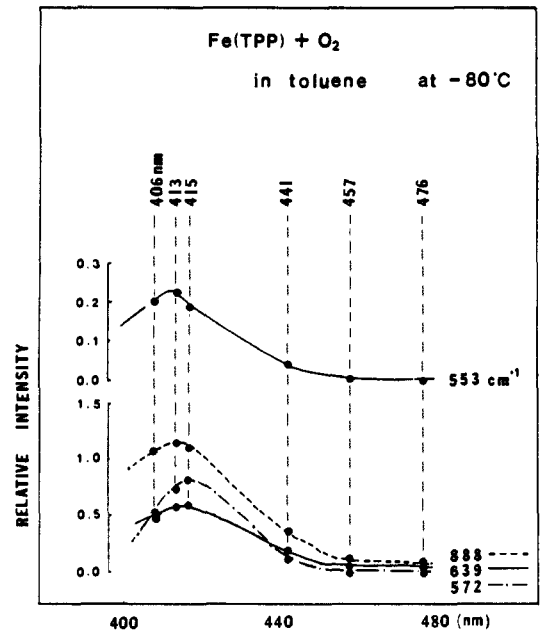

Figure 11. Raman excitation profiles obtained from a toluene solution of (TPP)Fe-^{18}O-^{18}O-Fe(TPP) at -80 °C.

Table III. Comparison of ν(Fe-O) for Various Species

porphyrins	temp, °C	ν(Fe-O), cm^{-1}	$\Delta\nu$, cm^{-1}	ref
$[Fe(TMP)]_2O_2$	-80	574 (547)	27	22
$[Fe(TPP)]_2O_2$	-80	577 (553)	24	*a*
$[Fe(OEP)]_2O_2$	-80	576 (550)	26	*a*
$[Fe(\alpha^4\text{-}T_{PIV}PP)]_2O_2$	-80	570 (547)	23	*a*
$[Fe(cis\text{-}\alpha^2\beta^2\text{-}T_{PIV}PP)]_2O_2$	-80	570 (547)	23	*a*
$[Fe(T(2,6\text{-}MeO)_4PP)]_2O_2$	-80	572 (550)	22	*a*
O=Fe(TPP)	-60	845 (812)	33	*a*
O=Fe(TMP)	-60	845 (812)	33	22, 38
O=Fe(OEP)	-60	845 (812)	33	*a*
$Fe(TPP)O_2$	25 K	509 (487)	22	4
$Fe(OEP)O_2$	25 K	510 (486)	24	*a*
$Fe(Pc)O_2$	15 K	488 (466)	22	41
Fe(TMP)(pip)O_2	-80	568 (545)	23	*a*
Fe(TPP)(pip)O_2	-80	575 (551)	24	19
Fe(OEP)(py)O_2	-80	573 (548)	25	*a*

[a] This work. [b] All work was done in toluene solution except for the five-coordinate oxygen adduct. The number in parentheses indicates the frequency of the ^{18}O species.

structure-sensitive; one pair is the bands at 1364 and 1556 cm^{-1} and the other is those at 1369 and 1564 cm^{-1}. These bands cannot be attributed to the unreacted Fe(II)(TPP)(intermediate spin) since the solution is saturated with dioxygen. Upon warming, the latter pair is weakened gradually and disappears at high temperature. Therefore, we attribute the bands at 1369 and 1564 cm^{-1} to the ferryl porphyrin containing the low-spin and +4 oxidation state.[6] The former pair at 1364 and 1556 cm^{-1} observed at low temperature (trace A) is assigned to the peroxo-bridged dimer, (TPP)Fe-O-O-Fe(TPP) containing the high-spin and +3 oxidation state. The bands at 1363 and 1554 cm^{-1} observed at 15 °C (trace E) are due to the μ-oxo dimer. Since the μ-oxo dimer also contains the high-spin and +3 state,[37] it is not possible to distinguish it from the peroxo-bridged species.

As stated earlier, the ν_s(Fe-O) of (TPP)Fe-O-O-Fe(TPP) was resonance-enhanced by 406.7-nm excitation. To examine the excitation profile of this mode, we measured the RR spectra with excitation lines from 406.7 to 676.4 nm. Figure 10 shows the RR spectra obtained with excitation lines at 406, 413, 415, 441, 457, and 476 nm. The spectra obtained with excitation above 476 nm are not shown because these lines yield no enhancement. Using the solvent band at 522 cm^{-1} as the internal standard, we plotted the relative intensities of four vibrations vs the exciting wavelength

in Figure 11. It shows the excitation profiles of the bands at 553 [ν_s(Fe-O) of the peroxo-bridged species], 572 (out-of-plane porphyrin deformation), 639 (phenyl mode), and 888 cm^{-1} (in-plane porphyrin deformation). It is seen that the intensities of these four bands maximize at 415-410 nm. Therefore, we conclude that the Soret π-π^* transition is responsible for resonance enhancement of the ν_s(Fe-O) of the peroxo-bridged dimer.

Oxidation of Other Iron Porphyrins. Similar experiments were carried out using several other porphyrins such as Fe(OEP), Fe(α^4-$T_{PIV}PP$),[9] Fe(*cis*-$\alpha^2\beta^2$-$T_{PIV}PP$), and Fe(T(2,6-MeO)$_4$PP) in order to observe five-coordinate dioxygen adducts of the $FePO_2$ type containing bulky porphyrins that might sterically hinder the formation of the peroxo-bridged species. In all cases, only the bands characteristic of the peroxo-bridged species were observed in solution at -80 °C and these solutions exhibited ferryl bands upon warming. In contrast to the NMR studies,[9] we could not observe the Raman spectra of "base-free" O_2 adducts of these porphyrins in toluene solution at -80 °C. This may be due to local heating caused by the laser beam. However, the Raman spectra of their O_2 adducts were observed in O_2 matrices at 15-30 K.[3,4,36] Table III lists the ν(Fe-O)/ν(FeO) of all the complexes thus far determined in our laboratory.

Acknowledgment. This work was supported by the National Science Foundation (Grant DMB-8613741). The Raman spectroscopic equipment used for this investigation was purchased with funds provided by a National Science Foundation grant (CHE-8413956). We thank Prof. J. R. Kincaid, Dr. L. M. Proniewicz, and Dr. R. Czernuszewicz (University of Houston) for their valuable comments.

Spin Polarization Conservation during Triplet-Triplet Energy Transfer in Fluid Solution As Studied by Time-Resolved ESR Spectroscopy

Kimio Akiyama,* Atsuko Kaneko, Shozo Tero-Kubota, and Yusaku Ikegami

Contribution from the Chemical Research Institute of Non-Aqueous Solutions, Tohoku University, Katahira 2-1-1, Sendai 980, Japan. *Received September 5, 1989*

Abstract: Electron spin polarization of pyridinyl radicals generated from the photosensitized dissociation of the dimers was studied. Addition of triplet sensitizer to the dimer solution induced drastic change in the CIDEP spectrum. Examinations of the dependence of spectral change on the T_1 state energy level and the spin alignment in the T_1 sublevels of sensitizers lead to the conclusion that energy transfer between the pyridinyl dimer and the sensitizer occurred and that the spin polarization was conserved during the process. From a series of triplet donors, nonphosphorescent T_1 states of two types of pyridinyl dimers were estimated to be 2.43 eV for the 2,2'-dimer of 1-methyl-4-*tert*-butylpyridinyl and 2.65 eV for the 4,4'-dimer of 1-methylpyridinyl.

Time-resolved ESR (TRESR) method has played an important role in studying photochemical reaction mechanisms because the CIDEP spectra give information about the character of the excited state associated with the reaction as well as the radical intermediate with short lifetime.[1]

Recently, we first proposed the conservation of electron spin polarization during the triplet-triple (T-T) energy transfer in fluid solution,[2] although the possibility had been demonstrated in single crystals[3-6] and glassy matrices.[7-9] In our study, the dimer of the 1,4-dimethylpyridinyl radical (**2**) was used as the energy acceptor, since direct photochemical excitation induced homolytic cleavage from the S_1 state, showing a pure RPM (radical pair mechanism) with A/E (absorptive/emissive) polarization in the ESR spectrum of the produced radical.[10] Addition of triplet sensitizers, such as 2-acetonaphthone and benzophenone, to the dimer solution caused a significant change of the CIDEP spectrum from A/E to all E polarization. In these sensitizers, the intersystem crossing (ISC) occurs preferentially to the highest triplet sublevel in the T_1 state with a high quantum yield. It was found that the occurrence of the polarization transfer depends on the energy level of T_1 state of the sensitizer. These results provide us a new field in the application of the CIDEP method to determine the T_1 state energy level in fluid solution.

In the present study, we examine the T-T energy transfer in detail using a series of sensitizers as the donor and the dimers of 1-methylpyridinyl (**1**) and 1-methyl-4-*tert*-butylpyridinyl (**3**) radicals as the acceptor.

These radicals each couple at 2- and 4-positions to form dimers, and the equilibrium between the radical and dimers tends overwhelmingly toward the dimers in the dark. The structure of the dimers depends on the bulkiness of the substituent at the 4-position of the pyridine ring. According to ^{1}H NMR measurements, the solution of **3** contains dl- and meso-2,2'-dimers (**5**)[11] and, for **2**, there are four kinds of isomers, dl- and meso-, 2,2'-, 2,4' and 4,4'-dimers. Only the 4,4'-dimer was observed for the solution of **1**. The ^{1}H NMR spectrum of the 4,4'-dimer (**4**) of **1** showed lines at δ_H values of 2.76 (6 H, NCH_3), 2.83 (2 H, 4,4'-H), 4.23 (4 H, 3,3'; 5,5'-H), and 5.79 (4 H, 2,2';6,6'-H) in CD_3CN with the Me_4Si standard at δ 0.00. All these dimers are photosensitive and generate the corresponding monomeric radicals from the S_1 states.[10,11] Positions of coupling in dimer formation have also been

(1) For a recent review, see: Trifunac, A. D.; Lawler, R. G.; Bartles, D. M.; Thurnauer, M. C. *Prog. React. Kinet.* **1986**, *14*, 43, and references therein.
(2) Akiyama, K.; Tero-Kubota, S.; Ikegami, Y.; Ikenoue, T. *J. Am. Chem. Soc.* **1984**, *106*, 8322.
(3) El-Sayed, M. A.; Tinti, D. S.; Yee, E. M. *J. Chem. Phys.* **1969**, *51*, 5721.
(4) Clarke, R. H. *Chem. Phys. Lett.* **1970**, *6*, 413.
(5) Scharnoff, M.; Hurbe, E. B. *Phys. Rev. Lett.* **1971**, *27*, 576.
(6) Kim, S. S.; Weissman, S. I. *Rev. Chem. Intermed.* **1979**, *3*, 107.
(7) Weir, D.; Wan, J. K. S. *J. Am. Chem. Soc.* **1984**, *106*, 427. Wan, J. K. S.; Dobkowski, J.; Turro, N. J. *Chem. Phys. Lett.* **1986**, *131*, 129. Wan, J. K. S. *Electronic Magnetic Resonance*, Weil, J. A., Ed.; Canadian Chemical Society: Ottawa, Canada, 1987; 599.
(8) Imamura, T.; Onitsuka, O.; Murai, H.; Obi, K. *J. Phys. Chem.* **1984**, *88*, 4028. Imamura, T.; Onitsuka, O.; Obi, K. *J. Phys. Chem.* **1986**, *90*, 6741. Obi, K.; Imamura, T. *Rev. Chem. Intermed.* **1986**, *7*, 225.
(9) Murai, H.; Yamamoto, Y.; I'Haya, Y. J. *Chem. Phys. Lett.* **1986**, *129*, 201.
(10) Akiyama, K.; Tero-Kubota, S.; Ikenoue, T.; Ikegami, Y. *Chem. Lett.* **1984**, 903.
(11) Akiyama, K.; Ishii, T.; Tero-Kubota, S.; Ikegami, Y. *Bull. Chem. Soc. Jpn.* **1985**, *58*, 3535. Akiyama, K.; Tero-Kubota, S.; Ikegami, Y.; Ikenoue, T. *J. Phys. Chem.* **1985**, *89*, 339.

0002-7863/90/1512-3297$02.50/0